Structure of Copolymers of Syndiotactic Polypropylene with Ethylene

Claudio De Rosa,*,† Finizia Auriemma,† Esther Fanelli,† Giovanni Talarico,† and Donatella Capitani‡

Dipartimento di Chimica, Università di Napoli "Federico II", Complesso Monte S.Angelo, Via Cintia, 80126 Napoli, Italy, and Servizio NMR-CNR Area della Ricerca di Roma, Via Salaria, km. 29.300, I-00016 Monterotondo S.R.M.C. P.10, Italy

Received June 24, 2002; Revised Manuscript Received December 12, 2002

ABSTRACT: A structural characterization of copolymers of syndiotactic polypropylene containing ethylene comonomeric units (PPET) in a wide range of concentrations (0.4−60 mol %) is presented. The copolymer samples are crystalline up to an ethylene content of 18−20 mol %. Ethylene units are partially included in the crystals of both as-prepared and melt-crystallized samples. As-prepared PPET samples basically crystallize in conformationally disordered modifications of form II of syndiotactic polypropylene (sPP) containing kink bands. The amount of kink bands defects, represented mainly by T_6G_2 sequences, increases with the ethylene content. These modifications are metastable and transform by crystallization from the melt into the most stable form I or form II, depending on the ethylene concentration. PPET samples having low ethylene content (up to 6−7 mol %) crystallize from the melt into the antichiral form I, even though disordered modifications of form I are always obtained. For higher ethylene contents, mixtures of crystals of forms I and II are obtained by crystallization from the melt. The fraction of form II increases with increasing the crystallization temperature and the ethylene content. The form II obtained by melt crystallizations does not present kink-band disorder, all chains being in the more stable $(T_2G_2)_n$ helical conformation. This is the first example of crystallization of the isochiral form II of sPP from the melt at atmospheric pressure.

Introduction

The development of metallocene catalysts for the polymerization of propylene has provided access to new polymer microstructures, and new polymeric materials having interesting physical properties, as for instance highly syndiotactic poly(α-olefins)[1,2] and syndiotactic copolymers of propylene with other α-olefins,[3−6] have been produced. Studies on the synthesis and characterization of syndiotactic copolymers of propylene with 1-butene,[3−9,11] ethylene,[3−6,10] 4-methyl-1-pentene,[3] and octene[12−15] have recently appeared in the literature. In particular, the effect of the presence of comonomeric units on the polymorphic behavior of syndiotactic polypropylene has been extensively investigated.[6−11]

Syndiotactic polypropylene (sPP) presents a complex polymorphic behavior,[16−28] complicated by the presence of structural disorder.[21,26,29−31] Four crystalline forms have been described so far (Figure 1). The most stable form I[18−21,24−26] and the metastable form II[16,24,27] are characterized by chains in a **s**(2/1)2 helical conformation, packed in orthorhombic unit cells. In the limit ordered structure of the stable form I right- and left-handed helical chains alternate along the *a* and *b* axes of the unit cell (Figure 1A),[18] whereas a fully isochiral packing of the 2-fold helices characterizes the structure of form II (Figure 1B).[16,24,27] The two metastable modifications, form III (Figure 1C) and form IV (Figure 1D), present chains in *trans*-planar[17,22] and $(T_6G_2T_2G_2)_n$[23] helical conformations, respectively.

The polymorphic behavior of sPP is further complicated by the fact that disorder in the conformation of the chains may be present in low-stereoregular samples of sPP, crystallized in form II by quench−precipitation from solutions.[29,30] This disorder corresponds to the presence of *trans*-planar portions of chains connecting longer portions in the ordered TTGG 2-fold helical conformation.[29−31] In the resulting structure shown in Figure 2, *trans*-planar defects are frozen in the crystals and clustered in planes producing the formation of kink bands, while the parallelism of helical portions of chains is preserved. In the ordered regions the chains in helical conformation are packed like in the form II, whereas in the defective regions the chains containing *trans*-planar sequences are packed like in the form IV of sPP (Figure 2).[23,28] These disordered structures presenting kink bands could be thought as metastable modifications intermediate between the limit ordered forms II and IV of sPP.

A preliminary structural characterization of syndiotactic copolymers of propylene with small content of ethylene (PPET) has shown that the presence of even a small amount of comonomeric ethylene units induces, in the as-prepared samples, the crystallization of conformationally disordered modifications of form II of sPP containing kink bands.[6,10] It has been demonstrated, by solid-state CPMAS NMR experiments on copolymer samples containing ^{13}C-enriched ethylene units, that the ethylene units are, at least in part, included in the crystalline regions of the PPET copolymers.[10] The disordered modifications with kink bands form more easily in the PPET copolymers than in the case of the sPP homopolymer because they are kinetically favored by the easier local formation of *trans*-planar sequences in the presence of ethylene units.[10] In fact, while in the case of the sPP homopolymer the formation of the kink-band structures is a rare event occurring only for low stereoregular samples, quench-precipitated from solutions, these disordered structures are observed for all as-prepared samples of the PPET copolymers with low ethylene content, analyzed so far.[6,10] These kink-band structures are, however, metastable also for the copoly-

† Università di Napoli "Federico II".
‡ Servizio NMR-CNR Area della Ricerca di Roma.

10.1021/ma020981v CCC: $25.00
Published on Web 02/19/2003

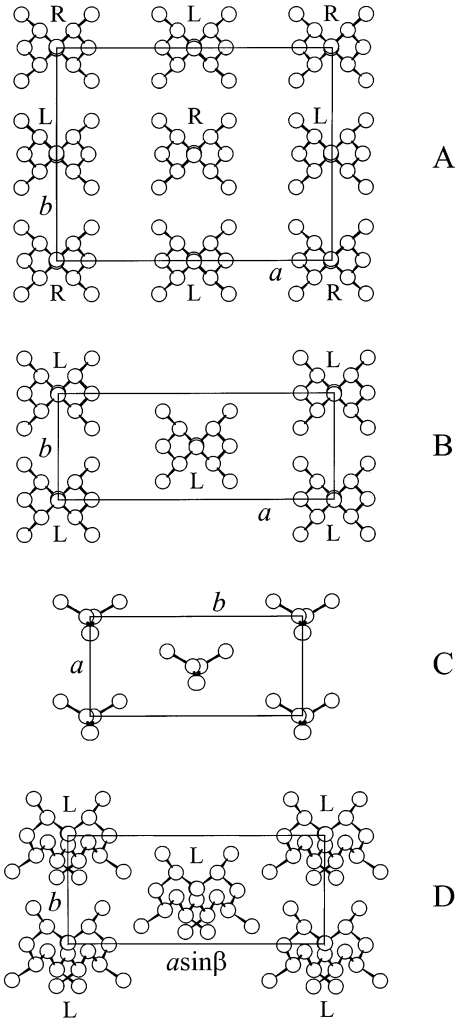

Figure 1. Models of packing of the limit ordered form I (A), form II (B), form III (C), and form IV (D) of sPP. R = right-handed helix; L = left-handed helix.

mers and transform into the more stable form I of sPP with chains in the ordered 2-fold helical conformation by thermal treatments or melt crystallization.[6]

It is worth noting that the structural characterization of PPET copolymers reported in the literature has been performed only for samples having very small concentrations of ethylene comonomeric units (in the range 0.4−2.6 mol %).[6,10] In this small range of composition the formation of the kink-band structures of sPP is driven by kinetic factors. In this paper the structural analysis of PPET copolymers is extended to samples having higher concentration of ethylene units in order to give new insights into the influence of the presence of ethylene on the polymorphism of sPP.

Experimental Section

Samples of PPET copolymers having concentration of ethylene in the range 0.4−60 mol % have been prepared using the single-center catalytic system composed of (phenyl)$_2$methylen(cyclopentadienyl)(9-fluorenyl)$ZrCl_2$ ($Ph_2C(Cp)(Flu)ZrCl_2$) and methylaluminoxane (MAO), according to the method described in ref 10. All copolymerizations were run at 10 °C in a 250 mL Pyrex reactor, agitated with magnetic stirrer, containing a toluene solution (100 mL) of the catalyst (2−3 mg) and MAO. The Al/Zr molar ratio was adjusted to 1000. Gas mixtures of ethylene and propene at the appropriate composition, prepared with vacuum line techniques and standardized by gas chromatography, were bubbled through the liquid phase at atmospheric pressure and a flow rate of 0.3 L/min. Under such conditions, total monomer conversions were lower than 10%, this ensuring a nearly constant feeding ratio. The copolymers were coagulated with excess methanol acidified with enough HCl (aqueous, concentrated) to prevent the precipitation of alumina from MAO hydrolysis, filtered, washed with further methanol, and vacuum-dried. Typical yields were 2−5 g with a 120 min reaction time. The conditions of polymerization for all PPET samples here analyzed are reported in Table 1.

The first three samples, PPET(1), PPET(2), and PPET(3), correspond to the three samples studied in the ref 10 contain-

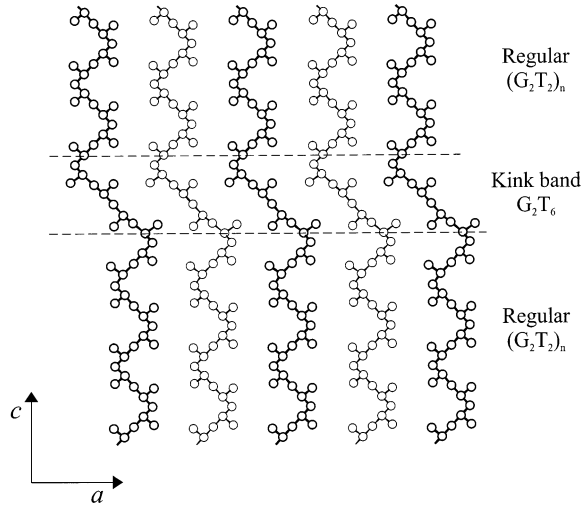

Figure 2. Model for the conformationally disordered modifications of form II of sPP containing kink bands. The chains are in a prevailing 2-fold helical conformation with defects characterized by *trans*-planar conformational sequences. The defective portions of the chains are clustered in planes, delimitated by the dashed lines, and correspond to conformational sequences G_2T_{4n+2} (in the figure $n = 1$). The chains are packed like in the form II of sPP, the helical portions of the chains being isochiral. The chains drawn with thick and thin lines are at $b = 0$ and 0.5, respectively.

Table 1. Composition, Melting Temperatures (T_m), Intrinsic Viscosities ([η]), and Molecular Weights (M_v) of PPET Copolymer Samples Prepared with the Catalytic Systems $Ph_2C(Cp)(Flu)ZrCl_2$/MAO and MePhC(Cp)(Flu)$ZrCl_2$/MAO[a]

sample	gas composition (mol % ethylene)	copolymer composition (mol % ethylene)	T_m (°C)	[η] (dL/g)	M_v[b]
PPET(1)	0.9	0.4	141.3	0.66	0.84×10^5
PPET(2)	2.4	1.5	136.3	0.69	0.88×10^5
PPET(3)	4.9	2.6	129.0	0.89	1.14×10^5
PPET(4)	7.6	6.3	110.2	1.78	2.37×10^5
PPET(5)	10.3	8.0	103.2	2.26	3.03×10^5
PPET(6)	12.1	8.5	95.0	1.94	2.59×10^5
PPET(7)	12.6	9.1	97.5	2.12	2.84×10^5
PPET(8)	15.4	9.8	93.7	2.10	2.80×10^5
PPET(9)	17.3	13.2	91.8	2.02	2.69×10^5
PPET(10)	21.4	14.3	78.2	1.13	1.45×10^5
PPET(11)	24.9	15.9	66.0	1.47	1.94×10^5
PPET(12)	27.1	16.2	65.9	1.47	1.94×10^5
PPET(13)	34.4	17.5	53.9	1.14	1.48×10^5
PPET(14)	45.5	26.8		1.17	1.53×10^5
PPET(15)	71.2	47.7		0.89	1.14×10^5
PPET(16)	82.5	59.1		1.01	1.31×10^5

[a] Temperature = 10 °C; pressure = 1 atm; solvent = toluene (100 mL); mole ratio Al/Zr = 1000; amount of catalyst = 2−3 mg; volume reactor = 250 mL; polymerization time = 2 h; flow rate = 5 mL/s; yield = 2−5 g. [b] The molecular weights have been calculated from the intrinsic viscosities using the parameters reported for atactic polypropylene: $\alpha = 0.96$ and $k = 1.24 \times 10^{-5}$ dL/g.[32]

ing 0.4, 1.5, and 2.6 mol % of ethylene-1-^{13}C comonomeric units (Isotec Inc., 99.+% isotopic purity), respectively. These samples were prepared with the same procedure and at the same temperature (10 °C) using (methyl)(phenyl)methylen(cyclopentadienyl)(9-fluorenyl)$ZrCl_2$ (MePhC(Cp)(Flu)$ZrCl_2$) as catalyst.[10]

Both used catalysts have been reported to be highly syndiotactic specific and highly regioselective (the amount of regioirregularities due to 2,1 insertions of propylene units being less than 0.1%).[10]

The composition of the copolymers was determined by analysis of the ^{13}C NMR spectra, recorded with a Varian XL-200 spectrometer operating at 50.3 MHz, of 10% w/v polymer solutions in deuterated tetrachloroethane (also used as internal standard) at 120 °C. The copolymers, according to this analysis, are random and homogeneous in the composition.

The compositions, the melting temperatures of the as-prepared powders, the intrinsic viscosities, and the molecular weights of the PPET samples are reported in Table 1. The melting temperatures were obtained with a differential scanning calorimeter Perkin-Elmer DSC-7 performing scans in a N_2 atmosphere at heating rate of 10 °C/min. The intrinsic viscosities were measured in tetrahydronaphthalene at 135 °C. The molecular weights were evaluated from the intrinsic viscosities using the parameters reported for atactic polypropylene.[32]

X-ray powder diffraction patterns were obtained at room temperature with an automatic Philips diffractometer using Ni-filtered Cu Kα radiation.

Solid-state ^{13}C NMR CPMAS spectra were recorded at room temperature on a Bruker AC-200 spectrometer, equipped with HP amplifier ^{1}H 200 MHz, 120 W continuous wave, and with a pulse amplifier M3205. The samples (50 mg) were packed into 4 mm zirconia rotors and sealed with Kel-F caps. The spin rate was kept at 8.0 kHz, and the 90° pulse was 3.0 μs. The contact time for the cross-polarization, optimized in order to maximize the signals in the rigid (crystalline) regions of the samples, was 1 ms; the relaxation delay time was 4 s. Spectra were obtained with 1024 points in the time domain, zero-filled, and Fourier-transformed with size of 2048 points; 7200 scans were performed for each sample. Crystalline polyethylene was used as external reference at 33.6 ppm from tetramethylsilane.

Results and Discussion

As-Prepared Samples. The X-ray powder diffraction profiles of the as-prepared crystalline samples of PPET are reported in Figure 3. The first three samples, PPET(1), PPET(2), and PPET(3), correspond to the samples analyzed in ref 10. The samples are crystalline up to a composition of 17−18 mol %, even though for these compositions the X-ray diffraction profiles show very broad reflections (profiles N and O of Figure 3), indicating the presence of a large amount of structural disorder. PPET samples with ethylene concentrations higher than 18−20 mol % are amorphous, as indicated by the X-ray diffraction patterns of the last three samples PPET(14)−PPET(16), not reported in Figure 3.

The X-ray diffraction profiles of Figure 3 indicate that all the crystalline PPET samples are basically crystallized in modifications close to the form II of sPP (Figure 1B). In fact, all the diffraction profiles are characterized by the presence of the 200 and 110 reflections at 2θ = 12.2° and 17°, respectively, typical of the isochiral form II.[16,24,27] The 020 reflection at 2θ = 16°, typical of the antichiral form I of sPP (Figure 1A), is generally absent or present only as a shoulder of the 110 reflection at 2θ = 17° (profiles F−I in Figure 3). For ethylene contents lower than 8 mol % (samples PPET(1)−PPET(5)) the 110 reflection at 2θ = 17° is relatively sharp (widths at half-height $\Delta 2\theta$ = 1°−1.5°, profiles A−E in Figure 3)

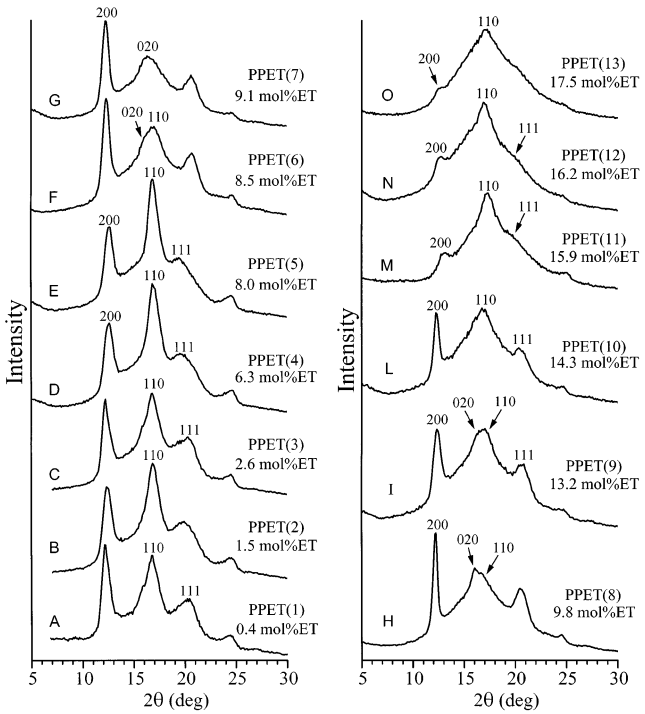

Figure 3. X-ray powder diffraction patterns of as-prepared PPET samples having the indicated ethylene (ET) content. The 200 reflection at 2θ = 12.2°, the 020 reflection at 2θ = 16°, typical of form I of sPP (b = 11.2 Å), the 110 reflection at 2θ = 17°, typical of the isochiral form II (b = 5.6 Å), and the 111 reflection (b = 5.6 Å) at 2θ = 20.7° are also indicated.

and broadens with increasing the ethylene content ($\Delta 2\theta$ = 2.5°−4°, profiles F−O in Figure 3).

These data indicate that, as already observed in the literature,[6,10] PPET samples crystallize mainly in form II with a certain amount of form I and variable amounts of disorder depending on the ethylene content. Samples with ethylene contents up to 7−8 mol % (samples PPET(1)−PPET(5)) crystallize basically in form II. For higher ethylene contents, the 110 reflection at 2θ = 17° shows a shoulder at 2θ = 16° (profile F in Figure 3), whose intensity increases with increasing the amount of ethylene (profiles F−H in Figure 3). This indicates that in the concentration range of 8−10 mol % of ethylene the copolymers crystallize in a mixture of forms II and I, and the amount of form I increases with increasing the ethylene content. The X-ray diffraction profile of the sample PPET(8) with 9.8 mol % of ethylene (profile H in Figure 3) presents in the range of 2θ = 15°−19° a maximum at 2θ = 16°, corresponding to the 020 reflection of form I.

For concentration of ethylene higher than 9.8 mol % the intensity of the 020 reflection at 2θ = 16° decreases (profile I in Figure 3), and the PPET samples with ethylene contents higher than 13 mol % crystallize again mainly in form II with a low amount of form I. The shoulder at 2θ = 16°, indeed, disappears for the samples PPET(11)−PPET(13) (profiles M−O in Figure 3). In these samples, besides the presence of a broad reflection centered at 2θ = 17°, a noticeable reduction of the 200 reflection at 2θ = 12° is observed (profiles M−O in Figure 3), which almost disappears in the X-ray diffraction profiles of the samples PPET(12) and PPET(13) with 16.2 and 17.5 mol % of ethylene, respectively (profiles N and O in Figure 3). This indicates that a high degree of disorder is present in these samples.

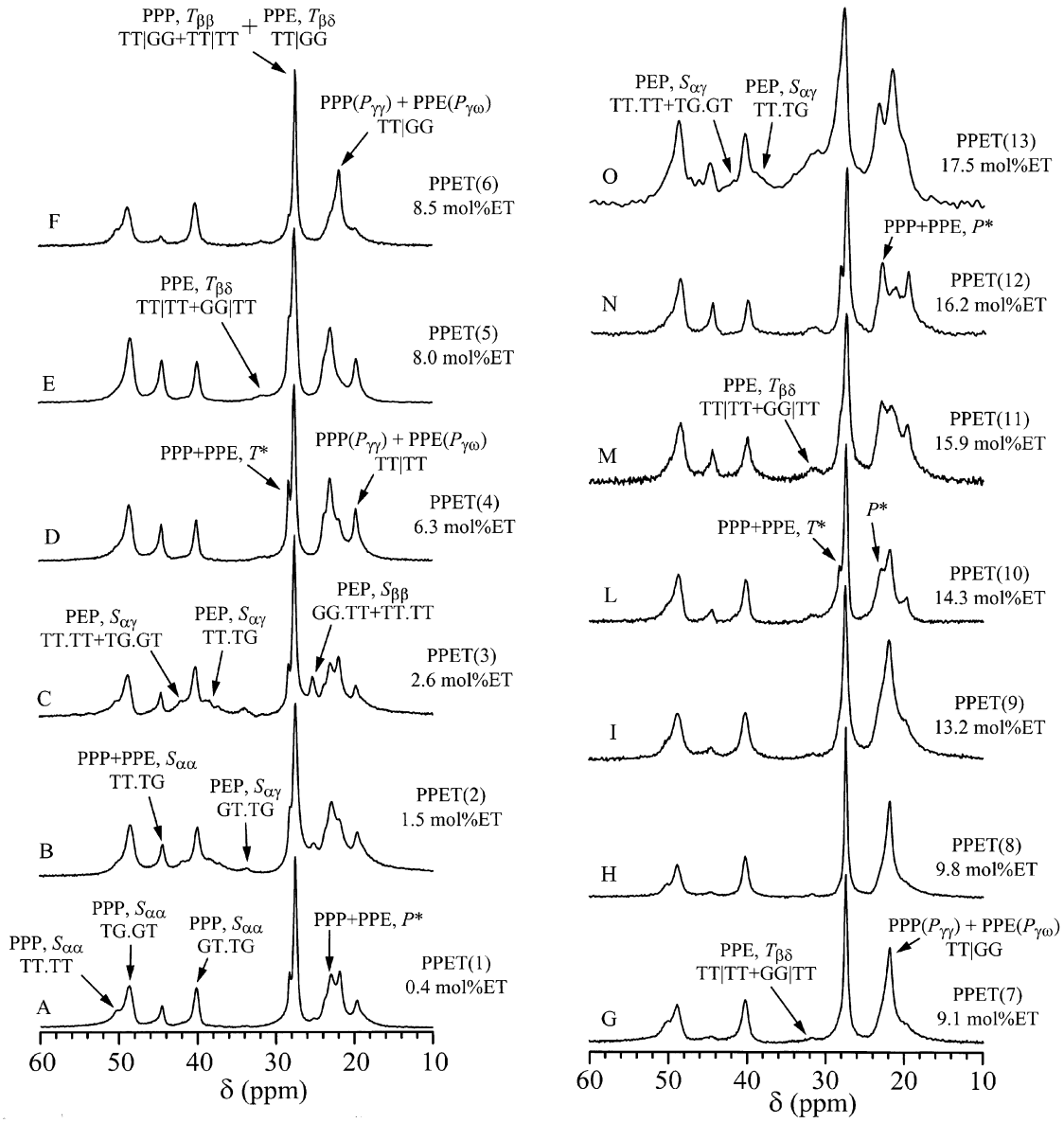

Figure 4. Solid-state ^{13}C NMR CPMAS spectra of the as-prepared samples of the PPET copolymers having the indicated ethylene (ET) contents. The assignment of the observed resonances to carbon atoms in the most probable constitutional sequence and conformational environment is also indicated.

The solid-state CPMAS ^{13}C NMR spectra of the PPET samples are reported in Figure 4. The spectra of the first three samples, PPET(1), PPET(2), and PPET(3) (Figure 4A−C), correspond to those reported in the ref 10. It is apparent that all the crystalline PPET samples, up to the ethylene content of 17−18 mol %, present similar CPMAS spectra (Figure 4A−O), even though the intensities of the observed resonances are not exactly the same in all the spectra. As discussed in the ref 10, these spectra present some features similar to those of the quench-precipitated sPP samples of refs 29 and 30 containing chains in disordered conformation. Most of the resonances observed in the spectra of Figure 4 do not scale with the ethylene concentration and are indicative of a nonordered conformation of the chains.

The assignment of the resonances observed in the spectra of the first three samples (Figure 4A−C) has been reported in the ref 10 (see Table 1 and Figures 3 and 4 of ref 10). The same resonances are observed in the spectra of the other crystalline PPET samples (Figure 4D−O), and the corresponding assignment is reported in Table 2. The spectra of Figure 4A−O are characterized by the usual resonances of methyl, at δ = 21.9 ppm, methine, at 27.4 ppm, and methylene carbon atoms, at 40.1 and 48.6 ppm, typical of the 2-fold $(T_2G_2)_n$ helical conformation of sPP,[33,34] and by additional resonances at δ = 19.6 and 22.9 ppm, for the methyl carbon atoms, and at δ = 44.5 and 50.2 ppm, for the methylene carbon atoms (Figure 4A−E,L−O). In particular, the resonance of the methylene carbon atoms at nearly 50 ppm is clearly present as a shoulder of the resonance at 48.6 ppm in the spectra of Figure 4A−C,F−O. Moreover, the resonances of the methyl carbon atoms at δ = 22.9 ppm and of the methine carbon atoms at δ = 27.4 ppm present shoulders at δ = 23.7 and 28.2 ppm, respectively (Figure 4A−E,L−O). As suggested in refs 29 and 30, these additional resonances could be attributed to the presence of conformational disorder in the crystalline phase, which originates from the presence of *trans*-planar sequences in chains having a prevailing 2-fold helical $(TTGG)_n$ conformation. In particular, the resonance at δ = 44.5 ppm was assigned

Table 2. Average Chemical Shifts of the Resonances Observed in the ^{13}C NMR CPMAS Spectra of As-Prepared PPET Copolymer Samples of Figure 4A−O (Samples PPET(1)−PPET(13))[a]

methylene atoms	constitutional sequence	conformational environment	observed chemical shifts (ppm)
$S_{\alpha\alpha}$	PPP and/or PPE	TT.TT	50.2
		TG.GT	48.6
		GT.TG	40.1
		GT.TT + TT.TG	44.5
$S_{\alpha\gamma}$	PEP	TT.TT + TG.GT	41.8
		GT.TT + TT.TG	38.5
		GT.TG	33.8
$S_{\beta\beta}$	PEP	TT.TT + GG.TT + TT.GG	25.2
methyl atoms[b]			
$P_{\gamma\gamma}$	PPP	TT|TT	19.6
$P_{\gamma\omega}$	PPE	TT|TT	
$P_{\gamma\gamma}$	PPP	TT|GG + GG|TT	21.9
$P_{\gamma\omega}$	PPE	TT|GG + GG|TT	
P*[b]	PPP + PPE	T′T′|G′G′ + G′G′|T′T′	22.9 + 23.7
methine atoms			
$T_{\beta\beta}$	PPP	TT|GG + GG|TT + TT|TT	27.4
$T_{\beta\delta}$	PPE	TT|GG	
T*[c]	PPP	T′T′|G′G′+G′G′|T′T′	28.2
	PPE	T′T′|G′G′	
$T_{\beta\delta}$	PPE	TT|TT + GG|TT	31.8

[a] The assignment of the observed resonances to carbon atoms in the most probable constitutional sequence and conformational environment is also reported. [b] The symbol ω identifies tertiary carbon atoms separated from the given nucleus by more than four bonds. [c] The symbols T′ and G′ indicate backbone torsion angles in a nearly *trans* and *gauche* conformation placed at interface between the *trans*-planar defective T_6 sequences and the portions of chains in G_2T_2 helical conformation.

to CH_2 groups in a TT.TG or GT.TT conformational environment, which experience one *γ-gauche* effect (the dots indicate the methylene carbon atoms), whereas the resonance at 19.6 and 50.2 ppm was assigned to methyl and methylene carbon atoms, respectively, in portions of chains in *trans*-planar TTTT conformation,[29] according to the resonance found by Sozzani et al. for the form III of sPP.[35] (Here in the following and in Figure 4, the vertical bar in the sequence TT|TT indicates the position of a tertiary or primary carbon atom, in the proper conformational environment.) Finally, the resonances at 22.9 ppm with its shoulder at 23.7 ppm (indicated with P* in Figure 4) and the shoulder at 28.2 ppm (indicated with T* in Figure 4) of the resonance at 27.4 ppm could be attributed to methyl (P standing for primary) and methine (T standing for tertiary) carbon atoms, respectively, belonging to PPP or PPE constitutional sequences, placed at the interface between the *trans*-planar and the helical portions of chains.

The presence of these additional resonances in the spectra of Figure 4 suggests that the as-prepared samples of the PPET copolymers are probably crystallized in conformationally disordered modifications, like, for instance, that shown in the model of Figure 2, described for the sPP homopolymer.[29] This model is only one of the possible structural models characterized by chains in disordered conformation containing *trans*-planar sequences.[29] It is worth noting that in the spectra of Figure 4 the intensities of the additional resonances at 50, 44.5, and 19.6 ppm are not all strictly related. In particular, the methylene resonance at 44.5 ppm is always present together with the resonance of the methyl groups at 19.6 ppm. The methylene resonance at ≈50 ppm is instead present in the spectra of Figure 4 even when the resonance at 44.5 ppm is absent or with very low intensity (for instance, Figure 4G−I). Therefore, the intensity of the resonance at ≈50 ppm, corresponding to methylene carbon atoms in TT.TT sequences, seems to be not related to those of the resonaces at 19.6 and 44.5 ppm.

Moreover, as already discussed in the ref 10, the intensities of the resonances at 19.6 and 44.5 ppm, indicative of the presence of *trans*-planar sequences, are similar to those observed in the sPP homopolymer (see Figure 3 in ref 29). This indicates that the resonances at 19.6 and 44.5 ppm are mostly due to methyl and methylene carbon atoms, respectively, belonging to propylene ...PPP... sequences. Therefore, the relative amount of *trans*-planar portions of chains does not scale with the ethylene concentration.

However, as shown in ref 10, the ethylene units are, at least in part, included in the crystalline phase of the copolymers, as clearly demonstrated by the presence in the spectra of the PPET samples containing ethylene-1-^{13}C comonomeric units (Figure 4C) of the resonances of small intensity at $\delta = 25.2$, 33.8, 38.5, and 41.8 ppm, all consistent with the presence of isolated ethylene comonomeric units (E) in fully syndiotactic propylene (P) sequences (...PEP...) and hence relative to secondary carbon atoms in suitable conformational environments[10] (Table 2). In fact, the signal at 25.2 ppm was assigned to secondary carbon atoms belonging to a PEP sequence symmetrically placed between two tertiary carbon atoms in the β positions (atoms $S_{\beta\beta}$, the symbol S standing for secondary carbon atoms), which always experience two *γ-gauche* effects regardless of the conformational environment.[10] The signals at 33.8, 38.5, and 41.8 ppm were assigned instead to methylene carbon atoms in PEP sequences, placed between two methine groups in the α and γ positions (atoms $S_{\alpha\gamma}$), in conformational environments GT.TG (two *γ-gauche* effects), TT.TG or GT.TT (a single *γ-gauche* effect), and TT.TT or TG.GT (zero *γ-gauche* effect), respectively[10] (Table 2 and Figure 4).

Therefore, the presence of ethylene comonomeric units in the crystalline regions of the PPET copolymers probably favors, locally, the formation of *trans*-planar sequences, which, in turn, should induce the crystallization of the samples in disordered modifications of form II containing kink bands. As shown in ref 29, the kink-band model of Figure 2 requires well-defined ratios between the intensities of the methylene resonances at 44.5 and 50.2 ppm and between the intensities of the resonances at 44.5 and 19.6 ppm. Each chain containing a kink-band G_2T_6 defect (Figure 2) comprises two methylene groups in a GT.TT conformational environment, giving the resonance at 44.5 ppm, one methylene group in a TT.TT sequence, one methylene carbon atom in a TG.GT sequence, and two methyl groups in TT|TT sequences, corresponding to the resonances at ≈50, ≈49, and 19.6 ppm, respectively. The ratio between the intensities of the resonances at 44.5 and ≈50 ppm should be nearly 2:1, whereas the ratio between the intensity of the methylene resonances at 44.5 and that of the resonance of the methyl groups in TT|TT sequences at 19.6 ppm should be nearly 1. These conditions are not fulfilled in all the spectra of Figure 4, since, as discussed before, the intensity of the resonance at ≈50 ppm seems to be not related to that of the resonances at 44.5 ppm. For this reason a quantitative analysis of the intensity of the resonances observed in the spectra of Figure 4 has been performed to verify the feasibility of the kink-band model.

The NMR spectra of Figure 4 have been fitted using up to 15 Lorentz curves, corresponding to the maxima of the observed NMR signals. The results obtained for three cases, i.e., samples PPET(5) (Figure 4E), PPET(6) (Figure 4F), and PPET(12) (Figure 4N), are illustrated in Figure 5. These samples are representative of the three different observed behaviors. In the spectrum of Figure 4E the resonance at ≈50 ppm seems absent or with very low intensity, while the resonance at 44.5 ppm has a strong intensity. In the spectrum of Figure 4F the intensity of the resonance at ≈50 ppm is higher than that of the resonance at 44.5 ppm, and finally, in the spectrum of Figure 4N the resonances at 44.5 and ≈50 ppm are both present. The chemical shifts of the maxima and the relative integral intensity, w_i, of the Lorentz curves used in the fit are reported in Table 3. The total fraction of secondary (f_S), tertiary (f_T), and primary (f_P) carbon nuclei detected in the experimental spectra are also indicated in Table 3; these values fairly approach the corresponding amount of carbon nuclei embedded in the rigid (crystalline) domains.

It is apparent from Table 3 that the ratio between the intensities of the resonances of methylene carbon atoms joining *trans*-planar and helical sequences (GT.TT sequences, peak 3 at 44.5 ppm and peak 6 at ≈38 ppm) and the intensity of the methylene groups in TT.TT sequences (peak 1 at ≈50 ppm), $(w_3 + w_6)/w_1$, is never 2:1, as required by the model of Figure 2. However, the signal at ≈50 ppm (peak 1) is always rather broad and is also present in spectra of PPET samples mainly crystallized in form I, showing only a very small resonance at 44.5 ppm (Figure 4F−I). As reported by Sozzani et al.,[34] the resonance at ≈50 ppm is also due to methylene carbon atoms belonging to the amorphous phase or to regions of material placed at the interface between crystalline and amorphous phases. On the other hand, this resonance has been found also in CPMAS spectra of sPP samples well-crystallized in the ordered form I[34] and attributed by Sozzani et al.[34] to methylene groups in well-defined TT.TT sequences in the amorphous phase or in regions embedded at the interface between crystalline and amorphous phases. The resonace at 50 ppm is, indeed, broad and of high intensity basically in low crystalline PPET samples (for instance, sample PPET(12), Figure 5C and Table 3). Therefore, this signal should not be taken into account for quantitative analyses.

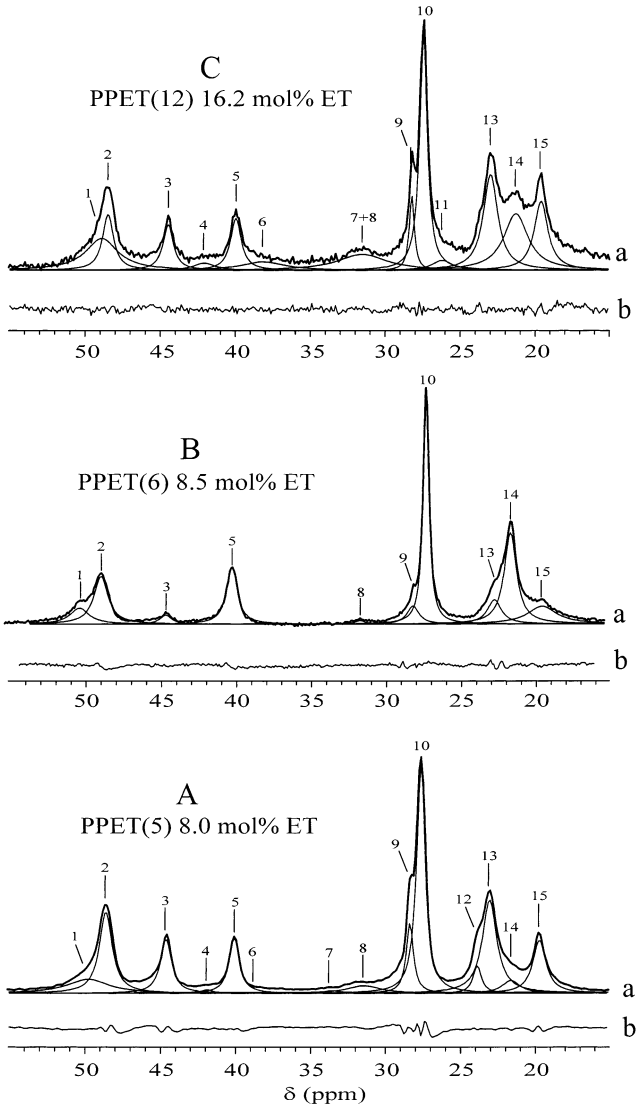

Figure 5. Fit of the solid-state ^{13}C NMR CPMAS spectra of as-prepared PPET(5) (A), PPET(6) (B), and PPET(12) (C) copolymer samples (curves a) with 15 Lorentz curves, corresponding to the observed resonance peaks. The peaks of the Lorentz curves are labeled with numbers from 1 to 15 in decreasing order of chemical shift. The differences between the experimental spectra (curves a) and the spectra simulated with the 15 Lorentz curves are also shown as curves b.

The data of Table 3 also indicate that in the spectra of Figure 5A,C (PPET(5) and PPET(12) samples containing a high amount of *trans*-planar sequences) the ratio between the intensities of the resonances of methylene carbon atoms in TT.TG sequences (peaks 3 and 6 at 44.5 and ≈38 ppm) and the intensity of the resonance of the methyl carbon atoms in TT|TT sequences at 19.6 ppm (peak 15), $(w_3 + w_6)/w_{15}$, is nearly 1, as required by the T_6G_2 kink-band model of Figure 2. This suggests that the average length of the *trans*-

Table 3. Results of Fitting of Experimental ^{13}C NMR CPMAS Spectra of Samples PPET(5), PPET(6), and PPET(12) with Lorentz Curves Centered around the Positions of the Maxima of Resonance Peaks[a]

				PPET(5) 8.0 mol % ET			PPET(6) 8.5 mol % ET			PPET(12) 16.2 mol % ET		
methylene atoms	constitutional sequence	conformational environment	peak n.i.	chem shift (ppm)	int (%) w(i)	f_S (%)	chem shift (ppm)	int (%) w(i)	f_S (%)	chem shift (ppm)	int (%) w(i)	f_S (%)
$S_{\alpha\alpha}$	PPP and/or PPE	TT.TT	1	49.7	7.3	∼35	50.1	5.8	∼32	49.0	10.1	∼34
		TG.GT	2	48.5	12.9		48.7	12.9		48.4	6.0	
		GT.TG	5	40.	7.4		40.1	11.7		40.0	5.5	
		GT.TT + TT.TG	3	44.5	7.0		44.5	2.0		44.5	4.7	
$S_{\alpha\gamma}$	PEP	TT.TT + TG.GT	4	41.8	∼0.3					42.0	1.6	
		GT.TT + TT.TG	6	38.7	<0.1					38.1	3.7	
		GT.TG	7	33.7	∼0.2					33.7	*b*	
$S_{\beta\beta}$	PEP	TT.TT + GG.TT + TT.GG	11							26.2	2.0	
methyl atoms						f_P (%)			f_P (%)			f_P (%)
$P_{\gamma\gamma}$	PPP	TT|TT	15	19.7	8.6	∼31	19.6	10.0	∼38	19.6	9.5	∼37
$P_{\gamma\omega}$	PPE	TT|TT										
$P_{\gamma\gamma}$	PPP	TT|GG + GG|TT	14	21.6	2.8		21.7	21.2		21.3	13.7	
$P_{\gamma\omega}$	PPE	TT|GG + GG|TT										
P*	PPP + PPE	T′T′|G′G′ + G′G′|T′T′	13	23.0	16.8		22.8	6.4		23.0	13.8	
			12	23.8	2.9							
methine atoms						f_P (%)			f_P (%)			f_P (%)
$T_{\beta\beta}$	PPP	TT|GG + GG|TT + TT|TT	10	27.6	24.3	∼34	27.3	25.4	∼30	27.5	17.8	∼29
$T_{\beta\delta}$	PPE	TT|GG										
T*	PPP	T′T′|G′G′ + G′G′|T′T′	9	28.3	6.2		28.1	4.1		28.2	3.7	
	PPE	T′T′|G′G′										
$T_{\beta\delta}$	PPE	TT|TT + GG|TT	8	31.4	3.2		31.6	0.6		31.5	7.8	

[a] The peaks are labeled with numbers in decreasing order of chemical shifts. The assignment of the resonances, as in Table 2, the chemical shifts of the maxima and the relative integral intensities (w_i) of the Lorentz curves, and the experimental total fraction of signals for CH_2 (f_S), CH_3 (f_P), and CH (f_T) carbon atoms are also reported. [b] This peak is broad and hidden by the maximum at 31.6 ppm (no. 8). In the fit a single broad peak, centered around 31.5 ppm, was considered.

planar sequences T_m is around $m = 6$, as in the model of Figure 2.

The sample PPET(6) (Figure 5B) contains only a small amount of *trans*-planar sequences. The resonance at 44.5 ppm (peak 3) is, indeed, weak and rather broad, while the resonances at 50 and 19.6 ppm are clearly observed (peaks 1 and 15, respectively). Also in this case the latter resonances are mainly due to carbon nuclei belonging to the amorphous phase or to interface regions between crystalline and amorphous phases.[34]

The quantitative analysis of Table 3 also shows that the ethylene units are in part included in the crystalline phase of the copolymers.[10] The molar fraction of ethylene units included in the crystals or in the rigid regions of the material placed at the interface between crystalline and amorphous phases may be evaluated as the ratio between the relative integral intensities of the resonances of methylene carbon atoms belonging to ethylene units (peaks 4, 6, and 7, PEP sequences) and the total amount of secondary nuclei f_S, i.e., $^1/_2(w_4 + w_6 + w_7)/f_S$. For instance, it corresponds in the case of the sample PPET(12) with 16.2 mol % of ethylene to nearly 8−9 mol %.

The formation of *trans*-planar sequences is probably favored, locally, by the presence in the crystals of ethylene units. The kinetically favored clustering of T_6G_2 sequences, like in the models of Figure 2, induces the crystallization in these disordered modifications, where the *trans*-planar sequences (TTTT or TTTG) do not necessarily occur in correspondence of the ethylene comonomeric units.

Even though the intensities of the resonances at 19.6, 22.9, and 44.5 ppm, indicative of the presence of *trans*-planar sequences, do not scale with the ethylene concentration, they change in the spectra of different PPET samples, indicating that the amount of kink-band defects is different in the various PPET copolymers. The amount of kink bands is maximum for the samples having ethylene concentration up to 7−8 mol % (the intensities of the resonances at 44.5 and 19.6 ppm is maximum, Figure 4A−E), whereas it is very small, almost negligible, for the samples having ethylene content in the range 8.5−10 mol % (the intensities of the resonances at 19.6 and 44.5 ppm are very small, Figure 4F−H). For higher ethylene concentration, in the range 13−18 mol %, the PPET samples show again an appreciable amount of kink-band defects (the spectra in Figure 4I−O present again the resonances at 19.6 and 44.5 ppm).

As discussed before, the ratio between the intensities of the resonances at 44.5 and 19.6 ppm is always nearly 1. This indicates that the increase of the amount of conformational disorder for as-prepared samples having ethylene units in the ranges 6−8 mol % (Figure 4D,E) and 16−18 mol % (Figure 4M−O), is, probably, mainly due to an increase of T_6G_2 sequences, breaking at random the regular $(T_2G_2)_n$ helical conformation, rather than to the formation of longer *trans*-planar sequences.

It is worth mentioning that the above-cited resonances at $\delta = 25.2$, 33.8, 38.5, and 41.8 ppm of $S_{\alpha\gamma}$ nuclei belonging to isolated ethylene units (PEP sequences) included in the crystalline regions, present in the CPMAS spectra of PPET samples containing ^{13}C-enriched ethylene (PPET(1)−PPET(3), Figure 4A−C), are less visible in the CPMAS spectra of the PPET samples containing low content of ethylene units with ^{13}C nuclei in the natural abundance (Figure 4D−M). They are instead clearly visible in the spectra of samples with higher ethylene contents (for instance, for the sample PPET(13) in Figure 4O).

With increasing the ethylene content, besides the appearance of these resonances of PEP methylene carbon atoms, a weak resonance at 31.8 ppm appears in the CPMAS spectra of the PPET samples (for instance, Figure 4E). The intensity of this signal increases with increasing the ethylene content (Figure 4M,N). This resonance is mainly related to methine carbon atoms belonging to ...PPEP... sequences (atoms $T_{\beta\delta}$) in *trans*-planar TT|TT or helical GG|TT conformational environments, which experience one *γ-gauche* effect less than the methine carbon atoms $T_{\beta\beta}$ in the PPP constitutional sequences, whose resonance occurs at 27.4 ppm (two *γ-gauche* effects). It is worth noting that the resonance of the methine carbon atoms $T_{\beta\delta}$ in ...PPEP... sequences in TT|GG conformation also occurs at 27.4 ppm (two *γ-gauche* effects, Table 2). The presence of the resonance at 31.8 ppm indicates that the isolated ethylene units are included in the crystalline phase, not necessarily in the disordered *trans*-planar regions but even in the ordered portion of chains in helical conformation.

A comparison between the X-ray diffraction profiles of Figure 3 and the solid state NMR of Figure 4 indicate that, when the PPET samples are crystallized prevailingly in form II (the X-ray diffraction profiles present only the 110 reflection at $2\theta = 17°$, Figure 3A−E,L−O), they present conformational disorder with kink-band defects (Figure 4A−E,L−O). When the samples crystallize partially, and/or prevailingly, in form I (the X-ray diffraction profiles present the 020 reflection at $2\theta = 16°$, Figure 3F−H), the amount of kink bands is negligible and the chains are basically in the helical conformation (Figure 4F−H).

These data confirm that the presence of ethylene comonomeric units in the crystalline regions of the PPET copolymers, even in a wide range of ethylene concentration, induces the crystallization of the samples in disordered modifications of form II containing kink bands (Figure 2). The formation of these disordered modifications is easier in the PPET copolymers than in the case of the sPP homopolymer because it is kinetically favored by the easier local formation of *trans*-planar sequences in the presence of ethylene units. As expected, the kink-band structures form also for high ethylene concentration (17−18%), compatible with the maintaining of the crystallinity. However, the data of Figure 4 indicate that the easiness of formation of kink bands, as well as the amount of kink-band defects, is not an increasing function of the ethylene content. In fact, as discussed above, kink-band defects are present in samples having low ethylene content, up to 8 mol % (samples PPET(1)−PPET(5), Figure 4A−E) and in samples with ethylene content higher than 13 mol % (samples PPET(10)−PPET(13), Figure 4L−O), but are absent for amounts of ethylene in the range 8−13 mol % (samples PPET(6)−PPET(9), Figure 4F−I). These results suggest that the crystallization of the disordered form II with kink bands for different ethylene concentrations is a result of a competition between kinetic factors, which favors the easy aggregation of *trans*-planar sequences, and the different thermodynamic stabilities of the antichiral form I and the isochiral conformationally disordered form II. This issue is analyzed in more detail in the next section where the structure of PPET copolymers has also been studied in samples crystallized isothermally from the melt in well-controlled conditions, which should favor the formation of the most thermodynamically stable structure.

It is worth noting that, in the X-ray diffraction profiles of PPET samples crystallized in the disordered form II with kink bands (for instance, Figure 3D,E), the intensities of the 200 and 111 reflections at $2\theta = 12.2°$ and 20.7°, respectively, are generally lower than those in the X-ray profiles of samples crystallized prevailingly in form I (for instance, Figure 3G,H). Moreover, it is apparent from Figure 3 that, for PPET samples crystallized in these disordered modifications, in the range 13−18 mol % of ethylene the intensities of the 200 and 111 reflections decrease with increasing the ethylene content (Figure 3I−O) and become very weak for the PPET(11)−PPET(13) samples with ethylene content in the range 16−18 mol % (Figure 3M−O). The X-ray diffraction profiles of the samples PPET(11)−PPET(13) (Figure 3M−O) are very similar to that of the *trans*-planar mesomorphic form of sPP, containing a small amount of crystals with chains in helical conformation.[36] The corresponding solid-state NMR spectra (Figure 4M−O) clearly indicate that the chains are not in the fully *trans*-planar conformation, like in the mesomorphic form, but in the helical conformation with kink-band defects. These samples are therefore not crystallized in the *trans*-planar mesomorphic form, but still in the disordered helical form II with kink bands. As shown in ref 31, disordered models of packing containing kink-band defects, like that of Figure 2, account for the reduction of the intensity of the reflections at $2\theta = 12.2°$ and 20.7° and for the increase of the amount of diffuse scattering subtending the Bragg reflections above the contribution of the amorphous phase. Therefore, the decrease of the intensities of these reflections in the samples of Figure 3M−O may be due to the increase of kink-band disorder. On the other hand, as discussed above, the increase of the amount of kink-band defects in these samples and in the samples of Figure 3D,E, is also clearly indicated by the enhanced intensities of the resonances at 44.5 and 19.6 ppm in the CPMAS spectra of Figure 4D,E,M−O.

Using the method described in the ref 31, we have calculated the X-ray diffraction profiles for models of disordered structure containing different amount of kink bands disorder, like that of Figure 2, and compared with the experimental X-ray diffraction profiles of Figure 3D,E,M−O. As shown in ref 31, the model of kink-band disorder of Figure 2, in the most general approach, is characterized by the statistical presence of $T_{4n+2}G_2$ (with $n = 1, 2, 3, ...$) conformational sequences along chains in helical $(T_2G_2)_n$ conformation (in Figure 2, the model with $n = 1$ is reported as an example). The probability that a G_2 conformational sequence is substituted by a T_2 sequence is indicated by the parameter $(1 - p)$. In this model, $p = 1$ corresponds to chains in fully ordered helical $(T_2G_2)_n$ conformation, whereas $p = 0$ corresponds

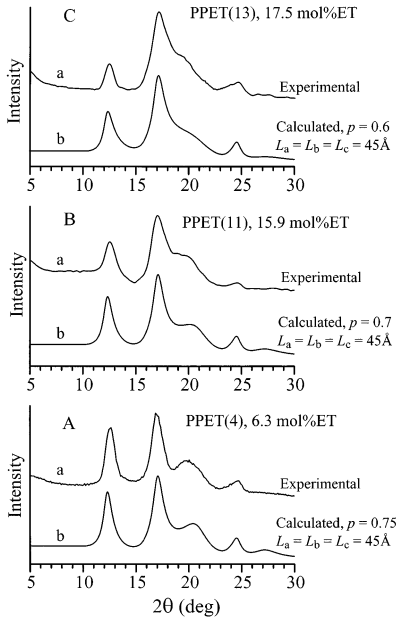

Figure 6. Experimental X-ray powder diffraction profiles (curves a) of the samples PPET(4) (A), PPET(11) (B), and PPET(13) (C) of parts D, M, and O of Figure 3, after the subtraction of the amorphous contribution and correction by the polarization factor, compared to the calculated X-ray diffraction profiles for models of kink-band disordered modifications of form II of the kind of Figure 2 (curves b). The values of the average size of the crystallites L_a, L_b, and L_c along the *a*, *b*, and *c* axes of the unit cell, assuming a Bernoullian statistic distribution of the crystallites sizes, and the values of the probability p used in the calculated profiles are also indicated.

to chains in fully *trans*-planar conformation. As shown in ref 31, the disordered conformations ($0 < p < 1$), expressed by the general formula ...$T_{4n+2}G_2$ $T_{4n'+2}G_2$ $T_{4n''+2}G_2$..., may crystallize if the *trans*-planar portions of the chains are clustered and the *gauche* bonds are all identically G^+ or G^-, producing isochiral helical sequences (Figure 2). The isochiral chains are packed like in the C-centered form II of sPP (Figure 1B). The average length of the fully *trans*-planar sequences in the macromolecular backbone $\langle L_{trans} \rangle$ is given, for any p, by $\langle L_{trans} \rangle = 2(2 - p)/p$.

The X-ray diffraction profiles of the samples PPET(4), PPET(11), and PPET(13) (Figure 3, D, N, and O, respectively) are reported in parts A, B, and C of Figure 6, respectively, after the subtraction of the amorphous contribution and correction by the polarization factor. These patterns are taken as representative examples of the X-ray diffraction profiles of the PPET samples of Figure 3. The calculated X-ray diffraction profiles for the disordered model of Figure 2, which give the best agreement with the experimental profiles, are also reported in Figure 6 (curves b). It is apparent that the diffraction profiles of the samples PPET(4), PPET(11), and PPET(13) are well reproduced by the kink-band disordered model of Figure 2 for $p = 0.75$ ($\langle L_{trans} \rangle = 3.3$ bonds, curve b of Figure 6A), $p = 0.7$ ($\langle L_{trans} \rangle = 3.7$ bonds, curve b of Figure 6B), and $p = 0.6$ ($\langle L_{trans} \rangle = 4.7$ bonds, curve b of Figure 6C), respectively. These results indicate that the X-ray diffraction data of the PPET samples are accounted for the kink-band disordered model of Figure 2, as also suggested by the NMR data of Figure 4, and that the amount of kink-band disorder increases with increasing the ethylene content. For the samples PPET(12) and PPET(13) the macromolecular chains are characterized by a nearly statistical presence of TG_2T and T_4 conformational sequences.

The X-ray diffraction profiles calculated for models of disorder containing *trans*-planar sequences in the kink bands not longer than T_6 ($n = 1$) are very similar to those of Figure 6. This indicates that both disordered models containing T_6G_2 kink-band sequences or *trans*-planar sequences longer than T_6 account for the X-ray powder diffraction profiles. The X-ray diffraction technique, therefore, does not allow distinguishing among different models of disorder. However, the ^{13}C NMR CPMAS analysis of the as-prepared PPET samples (Figures 4 and 5) has shown that the increase of kink-band disorder is mainly due to the increase of T_6G_2 sequences, which break the regular $(T_2G_2)_n$ helical conformation, rather than to the formation of longer *trans*-planar sequences. This result seems reasonable since disordered structural models containing kink bands with longer *trans*-planar sequences (of the kind T_{4n+2} with $n > 1$) would be at a higher cost of packing energy, because of the too low local density in the defective regions of the crystals. Therefore, the present analysis allows establishing that the portions of *trans*-planar chains embedded in the kink bands are probably never longer than T_6 in the PPET samples, as in the metastable form IV of sPP (Figure 1D), which is characterized, indeed, by chains in a regular $(T_2G_2T_6G_2)_n$ helical conformation. Therefore, as-prepared PPET samples with ethylene contents up to 18 mol % crystallize in a continuum of disordered modifications intermediate between the limit ordered forms II and IV of sPP (Figure 2).[37]

Melt-Crystallized Samples. The X-ray powder diffraction patterns of the as-prepared PPET samples and of the corresponding samples obtained by isothermal crystallizations from the melt at various temperatures T_c are reported in Figures 7−12. As discussed in the previous section, as-prepared samples of copolymers having low ethylene content, up to 8 mol %, are crystallized in the disordered form II with kink bands (Figures 7A−9A). It is apparent from Figures 7 and 8 that the same samples, up to 6−7 mol % of ethylene, instead, crystallize from the melt in the stable form I (Figure 1A), as indicated by the presence of the 020 reflection at $2\theta = 16°$ and the absence of the 110 reflection at $2\theta = 17°$ in the X-ray diffraction profiles of Figures 7B−F and 8B−E. As observed for the sPP homopolymer,[29] also for PPET copolymers with ethylene concentration up to 6−7 mol %, the disordered modification of form II (Figure 2) are metastable and can be obtained only in the as-prepared samples, by rapidly crystallization from the reaction medium. After melting and successive crystallization the antichiral stable form I is obtained (Figures 7B−F and 8B−E). At low crystallization temperatures disordered modifications of form I, characterized by a statistical disorder in the positioning of right- and left-handed helical chains, are formed, as demonstrated by the absence and/or low intensity of the 211 reflection at $2\theta = 18.8°$ in the X-ray powder diffraction patterns of Figures 7B-D and 8B−D.[26] We recall that for the sPP homopolymer the 211 reflection at $2\theta = 18.8°$ is typical of the packing characterized by the regular alternation of 2-fold helices of opposite chirality along the *a* and *b* axes (Figure 1A).[18] This reflection is present only in the X-ray diffraction patterns of the PPET samples crystallized at high temperatures, and its intensity increases with increasing the

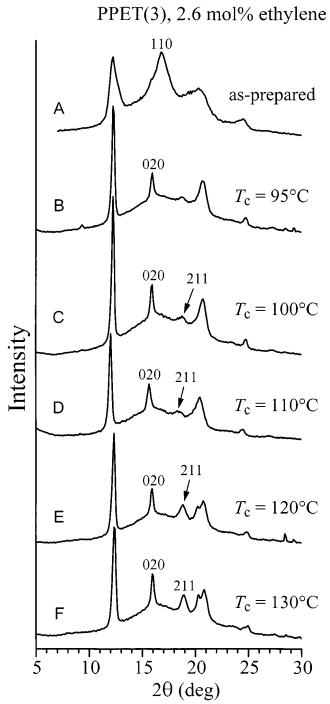

Figure 7. X-ray powder diffraction profiles of samples of the copolymer PPET(3) with 2.6 mol % of ethylene, isothermally crystallized from the melt at the indicated crystallization temperatures T_c. The 110 reflection at $2\theta = 17°$ of form II and the 020 and 211 reflections at $2\theta = 16°$ and 18.8°, respectively, of form I are also indicated.

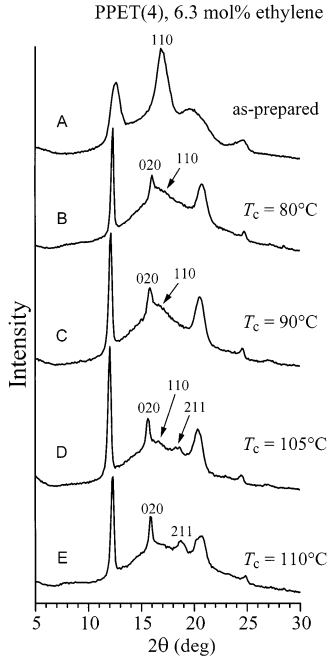

Figure 8. X-ray powder diffraction profiles of samples of the copolymer PPET(4) with 6.3 mol % of ethylene, isothermally crystallized from the melt at the indicated crystallization temperatures T_c. The 110 reflection at $2\theta = 17°$ of form II, and the 020 and 211 reflections at $2\theta = 16$ and 18.8°, respectively, of form I are also indicated.

crystallization temperature (Figures 7C−F and 8D−E). The profiles of Figures 7 and 8 indicate that, with increasing the crystallization temperature, crystals of form I of sPP, characterized by a certain degree of order in the alternation of right- and left-handed helices along the axes of the unit cell, are obtained. However, only

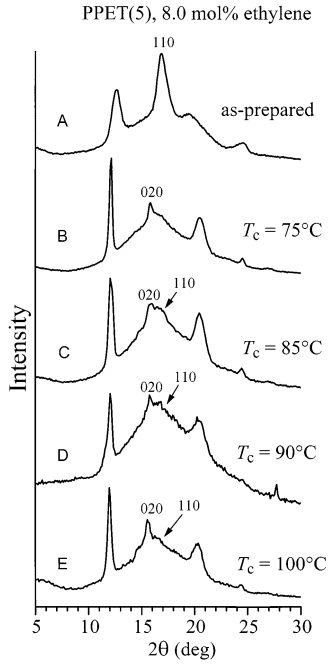

Figure 9. X-ray powder diffraction profiles of samples of the copolymer PPET(5) with 8.0 mol % of ethylene, isothermally crystallized from the melt at the indicated crystallization temperatures T_c. The 110 reflection at $2\theta = 17°$ of form II and the 020 reflection at $2\theta = 16°$ of form I are also indicated.

for PPET samples having very low content of ethylene (0.4−2.6 mol %), quite ordered modifications of form I of sPP are formed at high crystallization temperature (Figure 7F), but the intensity of the 211 reflection is still lower than that expected for the limit ordered structure of form I of s-PP.[26]

For PPET samples with ethylene content higher than 6−7 mol % the intensity of the 211 reflection is low or absent even at high crystallization temperatures (Figures 9−12). Already for a composition of 6.3 mol % of ethylene (sample PPET(4)) the intensity of the 211 reflection is very low and does not increase with increasing the crystallization temperature (Figure 8). For concentration of ethylene higher than 6.3 mol % the 211 reflection is always absent in the X-ray diffraction patterns of the melt-crystallized samples whatever the crystallization temperature (Figures 9−12). For these samples the ordering process in the alternation of right- and left-handed helices along the axes of the unit cell, typical of the sPP homopolymer,[18,26] does not occur.

The intensity of the 211 reflection at $2\theta = 18.8°$ can be used as a measure of the degree of order present in the crystals of form I. Precisely, since the intensity of the 020 reflection is constant with T_c, we use the ratio between the intensities of 211 and 020 reflections at $2\theta = 18.8°$ and 16°, respectively, $R = I(211)/I(020)$, to eliminate any dependence on the crystallinity and the thickness of the samples.[26]

The values of R of the PPET melt-crystallized samples are reported in Figure 13 as a function of the crystallization temperature and compared with the values of R of the sPP homopolymer taken from the ref 26. It is apparent that, while for the homopolymer the order parameter R increases with T_c from $R = 0$, corresponding to the limit disordered structure of form I, characterized by a statistical positioning of right- and left-handed helical chains in each site of the lattice, to a constant value $R \approx 1$, corresponding to the limit ordered

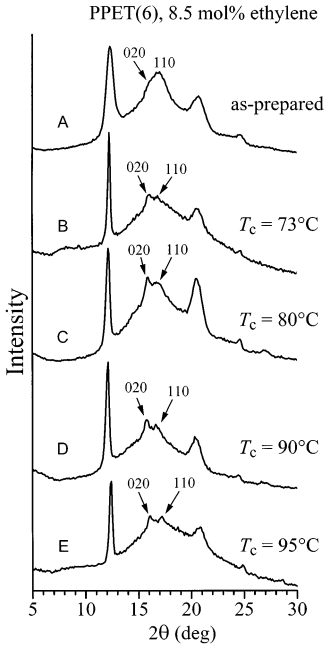

Figure 10. X-ray powder diffraction profiles of samples of the copolymer PPET(6) with 8.5 mol % of ethylene, isothermally crystallized from the melt at the indicated crystallization temperatures T_c. The 110 reflection at $2\theta = 17°$ of form II and the 020 reflection at $2\theta = 16°$ of form I are also indicated.

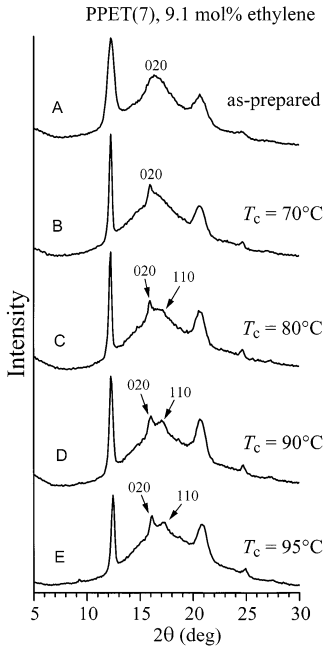

Figure 11. X-ray powder diffraction profiles of samples of the copolymer PPET(7) with 9.1 mol % of ethylene, isothermally crystallized from the melt at the indicated crystallization temperatures T_c. The 110 reflection at $2\theta = 17°$ of form II and the 020 reflection at $2\theta = 16°$ of form I are also indicated.

structure of form I of Figure 1A,[26] for the PPET copolymers the limit values of R are lower than 1 and decrease with increasing the ethylene content.

These data clearly indicate that the presence of small amounts of ethylene induces the crystallization of the disordered form II in the as-prepared PPET samples, and does not affect the usual crystallization from the melt of sPP in the most stable form I (Figure 1A), but prevents the formation of the ordered antichiral packing even at high crystallization temperatures. This behavior

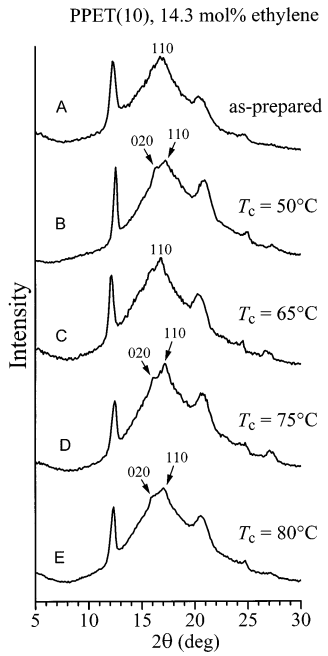

Figure 12. X-ray powder diffraction profiles of samples of the copolymer PPET(10) with 14.3 mol % of ethylene, isothermally crystallized from the melt at the indicated crystallization temperatures T_c. The 110 reflection at $2\theta = 17°$ of form II and the 020 reflection at $2\theta = 16°$ of form I are also indicated.

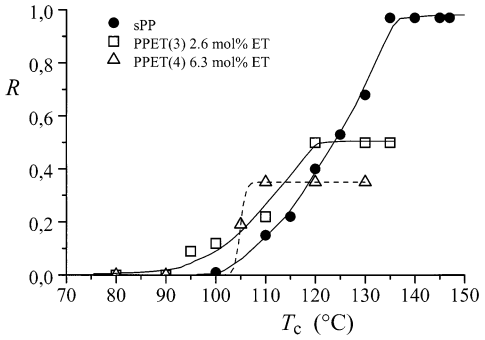

Figure 13. Values of the order parameter R of the PPET copolymer samples crystallized from the melt reported as a function of the crystallization temperature T_c and compared with the values of R of the sPP homopolymer taken from ref 26: (●) sPP; (□) PPET(3), 2.6 mol % of ethylene; (△) PPET(4), 6.3 mol % of ethylene.

can be easily explained considering that also in the copolymer samples crystallized from the melt the presence of ethylene in the crystals may induce the formation of a certain amount of form II or even produce the development of disorder in the stacking of *bc* layers of chains piled along *a*, characterized by shift of *bc* layers of *b*/4 along *b* (*b*/4 shifts disorder),[21,26] which in turn produces local arrangement of the chains as in the C-centered form II of sPP (Figure 1B). This is demonstrated by the presence in the X-ray diffraction profiles of the samples crystallized from the melt in form I of a broad diffraction peak at $2\theta = 17°$, corresponding to the 110 reflection (Figure 8B−E). This kind of disorder, observed also in the sPP homopolymer samples crystallized at low temperature,[21,26] destroys any correlation at long distances between the chirality of the helices along the *a* and *b* axes of the unit cell. Antichiral packing of first neighboring chains may still be preserved locally and lost in the long range because of the occurrence of the *b*/4 shifts disorder.

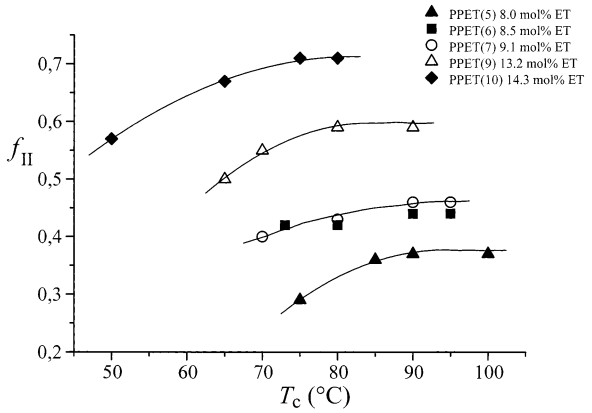

Figure 14. Values of the fraction of crystals of form II, f_{II}, for PPET copolymer samples crystallized from the melt reported as a function of the crystallization temperature T_c: (▲) PPET(5), 8.0 mol % ethylene; (■) PPET(6), 8.5 mol % ethylene; (○) PPET(7), 9.1 mol % ethylene; (△) PPET(9), 13.2 mol % ethylene; (◆) PPET(10), 14.3 mol % ethylene.

For PPET copolymers with ethylene content higher than 6−7 mol %, the X-ray diffraction profiles of the melt-crystallized samples show that the 211 reflection at $2\theta = 18.8°$ is always absent at any crystallization temperatures, whereas the 110 reflection at $2\theta = 17°$, typical of form II, appears with intensity which increases with increasing the crystallization temperature (Figures 9−12). Therefore, in the melt crystallizations, with increasing the crystallization temperature, the development of the 110 reflection, typical of form II (Figure 1B), is observed instead of that of the 211 reflection, typical of the ordered antichiral form I (Figure 1A). In particular, the sample PPET(5) with 8 mol % of ethylene, initially in form II (Figure 9A), crystallizes from the melt at low temperatures in disordered modifications of form I (Figure 9B), but at higher crystallization temperatures a certain amount of form II is obtained (Figure 9C−E). For higher ethylene concentration the amount of form II, obtained by melt crystallization, increases, as indicated by the comparable intensities of the 020 and 110 reflections at $2\theta = 16°$ and 17°, respectively, observed in the X-ray diffraction profiles of Figures 10 and 11. Even the sample PPET(7) with 9.1 mol %, which is initially mainly in form I (Figure 11A), crystallizes from the melt in form I at low temperatures (Figure 11B), whereas the form II develops at high crystallization temperatures (Figure 11D−E). This result is surprising since in the case of the sPP homopolymer the crystallization from the melt at atmospheric pressure of the isochiral form II (Figure 1B) has never been observed. For the sample PPET(10) with 14.3 mol % of ethylene the form II is always prevalent with respect to form I at any crystallization temperature (Figure 12).

The fraction of crystals of form II, obtained in the crystallization from the melt, may be evaluated from the relative intensities of the 110 and 020 reflections at $2\theta = 17°$ and 16°, respectively, as $f_{II} = I(110)/(I(110) + I(020))$. The values of f_{II} for the various PPET samples are reported in Figure 14 as a function of the crystallization temperature. The amount of form II increases with increasing the crystallization temperature and the concentration of ethylene. In these samples mixtures of crystals of forms I and II are obtained, and presumably, a high degree of *b*/4 shifts disorder is present in the crystals of form I. This means that local arrangements of the chains like in the C-centered form II of sPP (Figure 1B) may be also present in the crystals of form I.

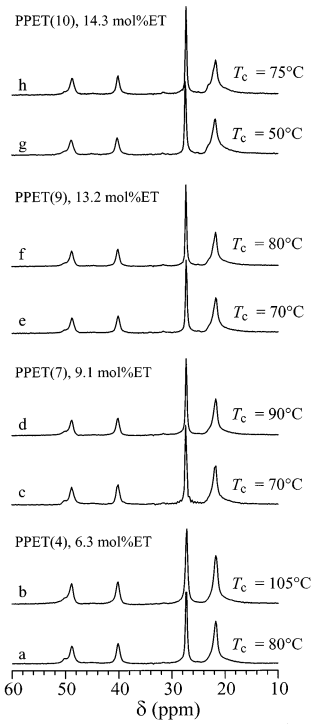

Figure 15. Solid-state ^{13}C NMR CPMAS spectra of samples of the PPET copolymers isothermally crystallized from the melt at the indicated temperatures: (a, b) PPET(4), 6.3 mol % ethylene; (c, d) PPET(7), 9.1 mol % ethylene; (e, f) PPET(9), 13.2 mol % ethylene; (g, h) PPET(10), 14.3 mol % ethylene.

Solid-state ^{13}C NMR spectra of the samples PPET(4), PPET(7), PPET(9), and PPET(10) crystallized from the melt at two different temperatures are reported in Figure 15. As shown in Figures 8, 11, 12, and 14, in these samples variable amounts of crystals of form II of sPP are present. It is apparent from Figure 15 that for all the melt-crystallized samples the CPMAS spectra present four sharp resonances of the methyl, methine, and methylene carbon atoms at $\delta = 21.9$, 27.4, and 40.1 and 48.6 ppm, respectively, indicating that the macromolecular chains are crystallized essentially in a $(T_2G_2)_n$ 2-fold helical conformation.[33,34] The resonances at 19.6 and 44.5 ppm, diagnostic of kink-band disorder, are absent, even in the case of the sample PPET(10) crystallized at 75 °C (Figure 15, curve h), which presents a fraction of crystals of form II of about 70% (Figures 12D and 14). These data indicate that the form II, which develops by melt crystallization of the PPET copolymer samples, is characterized by a regular helical $(T_2G_2)_n$ conformation. The presence of small signals at 25.2 and 33.8 ppm in the CPMAS spectra of Figure 15, due to $S_{\beta\beta}$ and $S_{\alpha\gamma}$ methylene carbon atoms belonging to PEP constitutional sequences, in TT.GG and GT.TG conformational environments, respectively, indicate that the ethylene units are included in the crystalline domains with chains in the regular helical $(TTGG)_n$ conformation.

The X-ray diffraction and NMR analyses of the PPET copolymer samples have shown that PPET copolymers crystallize from the melt in the form II without conformational disorder, with chains in the ordered helical $(TTGG)_n$ conformation (Figure 1B), whereas as-prepared samples crystallize in kink-band disordered modifications of form II (Figure 2). As in the case of the sPP

homopolymer, also for PPET copolymers the kink-band structures are metastable and transform into the conformationally ordered structures by crystallization from the melt.

The PPET copolymers analyzed in this paper provide the first example of crystallization of the isochiral form II of sPP from the melt at atmospheric pressure, for low undercoolings, and, hence, in conditions close to the thermodynamic equilibrium. For these materials, and high ethylene content, the isochiral form II of sPP is probably the thermodynamically stable modification, while for low ethylene contents the antichiral form I is still the most stable form. The ethylene units are partially included in the crystalline regions of the PPET copolymers and induce the kinetically favored formation of kink-band disordered modifications of form II in the as-prepared samples. These disordered modifications are metastable and do not crystallize from the melt. However, the presence of ethylene induces the crystallization of form II also in the melt-crystallized samples, this time without conformational kink-band disorder.

These results indicate that the ethylene units are probably better tolerated in the crystalline domains of sPP if the chains are locally packed as in the C-centered form II of sPP (Figure 1B). However, in the melt-crystallized samples mixtures of crystals of forms I and II are always obtained (Figures 7−12), and the fraction of form II increases with increasing the crystallization temperature and the ethylene content (Figure 14). Both crystals of forms I and II present disorder characterized by shifts of *bc* layers of chains along *b* by *b*/4 for form I and *b*/2 for form II ($b = 11.2$ Å for form I and 5.6 Å for form II; Figure 1A,B). Moreover, disorder characterized by the statistical substitution of right- and left-handed helical chains is present in both crystals of form I and form II. This disorder produces defects in the fully antichiral packing in the case of form I and departure from the fully isochiral packing in the case of form II. In this picture, chains containing longer propylene constitutional sequences basically crystallize in the form I of sPP. The presence of ethylene units as constitutional defects, included in these crystals, induces *b*/4 shifts disorder, which in turn prevents the crystallization of the most ordered antichiral modification of form I (Figure 1A). In fact, PPET copolymers with low ethylene contents crystallize from the melt basically in disordered modifications of form I (Figures 7 and 8). Portions of chains containing shorter fully propylene constitutional sequences, with high amounts of ethylene units, tend instead to crystallize mainly in the form II. These crystals include *b*/2 shifts disorder as well as disorder in the statistical substitution of right- and left-handed helical chains, but not kink-band disorder. These disorders produce local arrangements of the chains as in the antichiral form I and induce departures from the fully isochiral packing of the form II of sPP. This prevents the formation of kink-band disorder, which, in fact, requires an isochiral spiralization of the helical portions of the chains in the whole crystalline domain.[37,38] Fully isochiral modifications of form II of sPP, containing kink-band defects may crystallize only through a fast, cooperative kinetically controlled process;[38] they, therefore, develop only in the as-prepared PPET samples, rapidly crystallized from the reactor medium, and are inhibited when the samples crystallize from the melt under controlled conditions.

Concluding Remarks

As-prepared and melt-crystallized syndiotactic PPET copolymer samples have been characterized by X-ray diffraction and solid-state ^{13}C NMR spectroscopy. The samples are crystalline up to an ethylene concentration of about 18 mol %. The ethylene units are partially included in the crystals of both as-prepared and melt-crystallized samples.

Most of the as-prepared samples of these copolymers crystallize in conformationally disordered modifications of form II containing kink bands, characterized by portions of chains in *trans*-planar conformation in chains having a prevailing 2-fold helical conformation. Ethylene units are included in the disordered *trans*-planar portions as well as in the ordered helical portions of the chains. The presence of ethylene units induces the crystallization of these kink-band disordered modifications of form II. The formation of these disordered modifications is easier in the PPET copolymers than in the case of the sPP homopolymer because it is kinetically favored by the easier local formation of *trans*-planar sequences in the presence of ethylene units. The *trans*-planar sequences embedded in the kink bands are probably never longer than T_6 in the PPET samples, as in the metastable form IV of sPP, which is characterized, indeed, by chains in a regular $(T_2G_2T_6G_2)_n$ helical conformation. Different amounts of kink-band defects are present in the samples depending on the ethylene concentration. Even though the amount of *trans*-planar defects does not scale with the ethylene content, a high amount of T_6G_2 defects is present in the samples with high ethylene content (16−18 mol %). A continuum of disordered modifications intermediate between the limit ordered forms II and IV of sPP is present in the as-prepared PPET samples. These kink-band structures are metastable and transform by crystallization from the melt into the regular helical form I or form II, depending on the ethylene concentration.

The crystallization of the disordered form II with kink bands for different ethylene concentrations is a result of a competition between kinetic factors, which favors the easy aggregation of *trans*-planar sequences, and the different thermodynamic stabilities of the antichiral form I and the isochiral form II. Kink-band disordered structures are, indeed, obtained in the as-prepared samples with low ethylene contents, up to 8 mol %, and in samples with ethylene contents higher than 13 mol % but are absent for amounts of ethylene in the range 8−13 mol %. For low ethylene contents, up to 8 mol %, the kink-band structures are kinetically favored, while the most stable form is the antichiral form I. In these samples the few *trans*-planar sequences may easily aggregate in the fast crystallization process of the as-prepared samples, forming kink bands, which transform into the stable form I in the slow melt crystallization. The presence of ethylene, however, prevents the formation of the ordered fully antichiral form I, even for melt crystallizations at high temperatures.

For higher ethylene contents, in the range 8−13 mol %, kink-band structures are no longer obtained, and as-prepared samples basically crystallize in form I. This is probably due to the fact that the formation of kink-band structures, which occurs in a kinetically controlled fast crystallization, requires an isochiral spiralization of the helical portions of the chains and a clustering of the *trans*-planar portions of the chains in a highly cooperative process. The higher ethylene content in-

creases the flexibility of the macromolecular chains and the amount of *trans*-planar sequences. As a consequence, the clustering of the *trans*-planar portions as well as the cooperative isochiral spiralization of the helical sequences becomes more difficult. Crystallizations from the melt of these PPET samples having ethylene content in the range 8−13 mol % produce a mixture of crystals of forms I and II; the fraction of form II increases with increasing the crystallization temperature and the ethylene content. Form II obtained by melt crystallizations does not present kink-band disorder, all chains being in the more stable $(T_2G_2)_n$ helical conformation. These data indicate that in the range 8−13 mol % of ethylene concentration the antichiral form I is kinetically favored over the kink-band structures, whereas form II becomes thermodynamically more stable for high ethylene content.

As-prepared PPET copolymers with higher ethylene content, in the range 13−18 mol %, crystallize again in the disordered modifications of form II containing kink bands. The samples present a high amount of kink-band defects, essentially represented by many T_6G_2 sequences rather than longer *trans*-planar ones. In these cases, form I is probably destabilized because of the presence of too high amounts of constitutional defects in the macromolecular chains. On the other hand, even in the crystallizations from the melt of these samples, only a small amount of form I, in mixture with crystals of form II, is observed, form II being the prevalent modification at any crystallization temperature. Also in these cases, kink-band disorder is absent in the form II crystallized from the melt, the chains being in the stable $(T_2G_2)_n$ helical conformation. This is the first example of crystallization of the isochiral form II of sPP from the melt at atmospheric pressure. This confirms that at high ethylene concentration the form II becomes more stable; the formation of the antichiral form I is prevented both in the as-prepared and in the melt-crystallized samples for kinetic and thermodynamic reasons. Form I is, indeed, less stable because the high amount of constitutional defects produces the development of high amount of disorder in the stacking of *bc* layers of chains piled along *a*, characterized by shifts of the *bc* layers of *b*/4 along *b* (*b*/4 shift disorder), which in turn produces local arrangements of the chains as in the isochiral form II. Therefore, the increase of the thermodynamic stability of form II with respect to form I in PPET samples with increasing the amount of ethylene content is probably due to the fact that the ethylene units are better tolerated in the crystalline domains if the chains are locally packed as in the C-centered form II. The crystallization of the disordered kink-band modifications of form II in the as-prepared samples of PPET copolymers with high ethylene content, in the range 13−18 mol %, is still due to the fact that these structures are kinetically favored. In fact, while for ethylene content in the range 8−13 mol % the clustering of the *trans*-planar portions of chains and the cooperative spiralization of the helical sequences is a difficult process, slower than the crystallization of the defective form I, for higher ethylene content (>13 mol %), the amount of the *trans*-planar portions of chains is so high that the crystallization of kink-band structures is the only possible, relatively fast, process.

Both form I and form II crystallized from the melt in the PPET copolymer samples show structural disorder characterized by stacking faults in the piling of consecutive *bc* layers of $(T_2G_2)_n$ helical chains along *a* and disorder in the statistical substitution of right- and left-handed helical chains. These disorders induce departures from the fully antichiral packing of the helices in the crystalline domains of form I and departures from the fully isochiral packing of the helices in the crystalline domains of form II. In this latter case, the development of disorder in the substitution of right- and left-handed helices prevents the formation of kink-band structures in the crystallization from the melt, which requires the isochiral spiralization of the helical portions of the chains and, indeed, occurs only in the kinetically controlled crystallization of the as-prepared samples.

Acknowledgment. Financial support from the "Ministero dell'Università e della Ricerca Scientifica e Tecnologica" (PRIN 2000 and Cluster C26) is gratefully acknowledged.

References and Notes

(1) Ewen, J. A.; Jones, R.; Razavi, A.; Ferrara, J. D. *J. Am. Chem. Soc.* **1988**, *110*, 6255.
(2) Albizzati, E.; Resconi, L.; Zambelli, A. Eur. Pat. Appl. 387609 (Himont Inc.), 1991; *Chem. Abstr.* **1991**, *114*, 62980a.
(3) Galimberti, M.; Albizzati, E.; Mazzocchi, R. U.S. Patent 5196496, 1993.
(4) Kakugo, M. *Macromol. Symp.* **1995**, *89*, 545.
(5) Naga, N.; Mizunuma, K.; Sadatoshi, H.; Kakugo, M. *Macromolecules* **1997**, *30*, 2197; *Polymer* **2000**, *41*, 203.
(6) De Rosa, C.; Auriemma, F.; Vinti, V.; Grassi, A.; Galimberti, M. *Polymer* **1998**, *39*, 6219.
(7) De Rosa, C.; Talarico, G.; Caporaso, L.; Auriemma, F.; Fusco, O.; Galimberti, M. *Macromolecules* **1998**, *31*, 9109.
(8) De Rosa, C.; Auriemma, F.; Caporaso, L.; Talarico, G.; Capitani, D. *Polymer* **2000**, *41*, 2141.
(9) De Rosa, C.; Auriemma, F.; Orlando, I.; Talarico, G.; Caporaso, L. *Macromolecules* **2001**, *34*, 1663.
(10) De Rosa, C.; Auriemma, F.; Talarico, G.; Busico, V.; Caporaso, L.; Capitani, D. *Macromolecules* **2002**, *35*, 1314.
(11) Zhang, B.; Yang, D.; De Rosa, C.; Yan, S. *Macromolecules* **2002**, *35*, 4646.
(12) Jungling, S.; Mulhaupt, R.; Fisher, D.; Langhauser, F. *Ang. Makromol. Chem.* **1995**, *229*, 93.
(13) Thomann, R.; Kressler, J.; Mulhaupt, R. *Macromol. Chem. Phys.* **1997**, *198*, 1271.
(14) Thomann, R.; Kressler, J.; Mulhaupt, R. *Polymer* **1998**, *39*, 1907.
(15) Hauser, G.; Schmidtke, J.; Strobl, G. *Macromolecules* **1998**, *31*, 6250.
(16) Corradini, P.; Natta, G.; Ganis, P.; Temussi, P. A. *J. Polym. Sci., Part C* **1967**, *16*, 2477.
(17) Natta, G.; Peraldo, M.; Allegra, G. *Makromol. Chem.* **1964**, *75*, 215.
(18) Lotz, B.; Lovinger, A. J.; Cais, R. E. *Macromolecules* **1988**, *21*, 2375.
(19) Lovinger, A. J.; Lotz, B.; Davis, D. D. *Polymer* **1990**, *31*, 2253.
(20) Lovinger, A. J.; Davis, D. D.; Lotz, B. *Macromolecules* **1991**, *24*, 552.
(21) Lovinger, A. J.; Lotz, B.; Davis, D. D.; Padden, F. J. *Macromolecules* **1993**, *26*, 3494.
(22) Chatani, Y.; Maruyama, H.; Noguchi, K.; Asanuma, T.; Shiomura, T. *J. Polym. Sci., Part C* **1990**, *28*, 393.
(23) Chatani, Y.; Maruyama, H.; Asanuma, T.; Shiomura, T. *J. Polym. Sci., Polym. Phys.* **1991**, *29*, 1649.
(24) De Rosa, C.; Corradini, P. *Macromolecules* **1993**, *26*, 5711.
(25) De Rosa, C.; Auriemma, F.; Corradini, P. *Macromolecules* **1996**, *29*, 7452.
(26) De Rosa, C.; Auriemma, F.; Vinti, V. *Macromolecules* **1997**, *30*, 4137.
(27) De Rosa, C.; Auriemma, F.; Vinti, V. *Macromolecules* **1998**, *31*, 7430.
(28) Auriemma, F.; De Rosa, C.; Ruiz de Ballesteros, O.; Vinti, V.; Corradini, P. *J. Polym. Sci., Polym. Phys. Ed.* **1998**, *36*, 395.
(29) Auriemma, F.; Born, R.; Spiess, H. W.; De Rosa, C.; Corradini, P. *Macromolecules* **1995**, *28*, 6902.
(30) Auriemma, F.; Lewis, R. H.; Spiess, H. W.; De Rosa, C. *Macromol. Chem.* **1995**, *196*, 4011.

(31) Auriemma, F.; De Rosa, C.; Ruiz de Ballesteros, O.; Corradini, P. *Macromolecules* **1997**, *30*, 6586.
(32) Brandrup, J.; Immergut, E. H.; Grulke, E. A. *Polymer Handbook;* John Wiley: New York, 1999.
(33) Bunn, A.; Cudby, E. A.; Harris, R. K.; Packer, K. J.; Say, B. J. *J. Chem. Soc., Chem. Commun.* **1981**, 15.
(34) Sozzani, P.; Simonutti, R.; Galimberti, M. *Macromolecules* **1993**, *26*, 5782.
(35) Sozzani, P.; Galimberti, M.; Balbontin, G. *Makromol. Chem. Rapid Commun.* **1993**, *13*, 305.
(36) Nakaoki, T.; Ohira, Y.; Hayashi, H.; Horii, F. *Macromolecoles* **1998**, *31*, 2705.
(37) De Rosa, C.; Auriemma, F. *Macromol. Symp.* **2001**, *175*, 215.
(38) Lotz, B.; Mathieu, C.; Thierry, A.; Lovinger, A. J.; De Rosa, C.; Ruiz de Ballesteros, O.; Auriemma, F. *Macromolecules* **1998**, *31*, 9253.

MA020981V